M-2024

J. Chem. Thermodynamics **1987**, 19, 113–123

Thermophysics of metal alkanoates

VII. Heat capacities and thermodynamic properties of potassium *n*-butanoate[a]

P. FRANZOSINI,†

C.N.R. c/o Dipartimento di Chimica Fisica, Universita di Pavia, Viale Taramelli 16, I-27100 Pavia, Italy

S. P. NGEYI, and E. F. WESTRUM, JR.

Department of Chemistry, University of Michigan, An Arbor, Michigan 48109, U.S.A.

(Received 18 April 1986)

The subambient heat-capacity curve of potassium *n*-butanoate as determined by adiabatic equilibrium calorimetry is characterized by a "bifurcated" transition whose "peaks" occur at 123.85 and 142.3 K. The corresponding $(C_{p,m}/R)_{max}$, $\Delta_{trs}H^{\circ}_{m}/R$, and $\Delta_{trs}S^{\circ}_{m}/R$ values are 24.1, 23.85; 49.3 K, 32.5 K; and 0.400, 0.226, respectively. Smoothed thermodynamic functions are provided in tabular form from 10 to 350 K.

1. Introduction

Information (obtained by equilibrium adiabatic calorimetry) was provided in Papers III[1] and IV[2] of this series on the molar heat capacities (and relevant thermodynamic functions) of potassium propanoate and isobutanoate, respectively, in the temperature range between 5 and 350 K. Investigation is now extended to *n*-butanoate because of its peculiar thermophysical behavior which makes it a quite special member of the potassium *n*-alkanoate family.

Superambient d.s.c. results reported previously by one of us[3–6] on transition (trs), fusion (fus), and clearing (clr) temperatures and molar enthalpy changes for the sequence; potassium methanoate ($n_C = 1$; n_C: number of carbon atoms), ..., *n*-eicosanoate ($n_C = 20$) are shown in figure 1, where the sets of entropy changes specified below are plotted against n_C for $1 \leqslant n_C \leqslant 15$.

In figure 1 ○ represents $\Delta_{fus}S^{\circ}_{m}/R$, and T_{fus} is identified as the temperature at which one of the following transformations occurs:

Crystal = isotropic liquid	(for $1 \leqslant n_C \leqslant 3$);
Crystal = liquid crystal	(for $4 \leqslant n_C \leqslant 8$);
Plastic crystal = liquid crystal	(for $9 \leqslant n_C \leqslant 15$).

[a] The first paper in this series is reference 12.

† Died 24 January 1986.

0021-9614/87/020113+11 $02.00/0

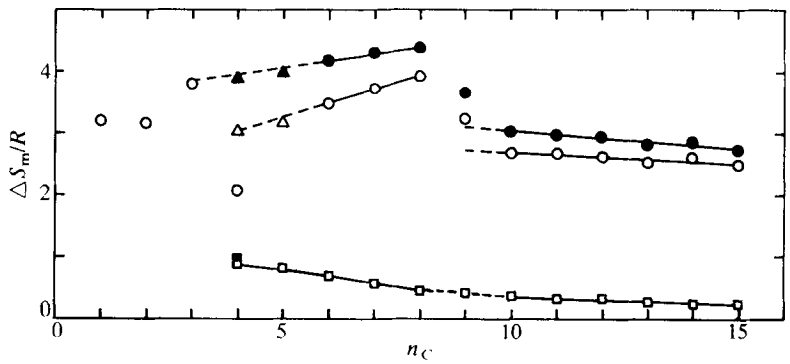

FIGURE 1. Entropy changes involved in various phase transformation of the potassium *n*-alkanoates with $1 \leqslant n_C \leqslant 15$. □, Clearing; ○, fusion; ▲, ●, summation of values for fusion and for clearing (see the text).

Among the $\Delta_{fus}S^\circ_m/R$s no correlation is apparent for $1 \leqslant n_C \leqslant 4$, whereas linear correlations exist, on the one hand, for $6 \leqslant n_C \leqslant 8$, and, on the other hand, for $10 \leqslant n_C \leqslant 15$. This indicates that each of these two groups of homologs probably has related, though different, fusion processes.

$\Delta_{fus}S^\circ_m/R$ for $n_C = 5$ is not known, inasmuch as transformational enthalpy increments for fusion and a close-to-fusion transition could not be resolved.[5]

The $\Delta_{fus}/S^\circ_m/R$ break between $n_C = 8$ and $n_C = 9$ is due to the change of the fusion process consequent on the formation of plastic crystalline phases at $n_C = 9$. The value for $n_C = 9$[4] was probably overestimated, because of the difficulty of an accurate evaluation occasioned by partial overlapping (in the recorded d.s.c. traces) of the (crystal = plastic crystal) "hump" and the fusion "peak": this value, if correctly measured, would probably lie on the extension to lower n_C of the $\Delta_{fus}S^\circ_m/R$ curve for $10 \leqslant n_C \leqslant 15$.

The lowest $\Delta_{fus}S^\circ_m/R$ value of the sequence is that shown by the *n*-butanoate.

Visual polythermal observations allowed Sokolov,[7] and Sokolov and Pochtakova[8] to claim for potassium *n*-butanoate the following phase transformations in the superambient region:

$$\text{Crystal III} \underset{(463\pm1)\ \text{K}}{\overset{T_{\text{III}\to\text{II}}}{\rightleftharpoons}} \text{crystal II} \underset{(555.5\pm2.5)\ \text{K}}{\overset{T_{\text{II}\to\text{I}}}{\rightleftharpoons}} \text{crystal I} \underset{(618\pm1)\ \text{K}}{\overset{T_{fus}}{\rightleftharpoons}} \text{liquid crystal} \underset{(677\pm1)\ \text{K}}{\overset{T_{clr}}{\rightleftharpoons}} \text{isotropic liquid.} \quad (1)$$

To avoid confusion, the nomenclature adopted in scheme (1) is that which we employ usually; in the original papers, however, the transformations at (618 ± 1) and (677 ± 1) K had been designated as a "transition" and "fusion", respectively.

Later the (superambient) phase relations listed in table 1 were obtained by d.s.c.[3] These differ from those reported elsewhere in that d.s.c. proved that both of the solid-state transformations mentioned by the Russian authors[7,8] are actually

TABLE 1. Superambient phase transformations (trf) of potassium *n*-butanoate as detected by d.s.c.[3]

trf	T_{trf}/K	$\langle T_{trf} \rangle$/K	$\Delta_{trf} S_m/R$
clr	677.3 ± 0.5	—	0.38
fus	626.1 ± 0.5	—	2.08
II → I [a]	562.2 ± 0.5 541 ± 1	552 ± 1	0.97 [b]
III → II [a]	467.2 ± 0.5 461.4 ± 0.5	464.3 ± 0.5	0.30 [b]

[a] Twin transformation (for explanation, see text).
[b] Cumulative value.

split into two component peaks. Accordingly, scheme (1) should be modified as follows:

$$\text{Crystal V} \underset{(461.4\pm0.5)\ \text{K}}{\overset{T_{V\to IV}}{\rightleftharpoons}} \text{crystal IV} \underset{(467.2\pm0.5)\ \text{K}}{\overset{T_{IV\to III}}{\rightleftharpoons}} \text{crystal III} \underset{(541\pm1)\ \text{K}}{\overset{T_{III\to II}}{\rightleftharpoons}} \text{crystal II}$$

$$\underset{(562.2\pm0.5)\ \text{K}}{\overset{T_{II\to I}}{\rightleftharpoons}} \text{crystal I} \underset{(626.1\pm0.5)\ \text{K}}{\overset{T_{fus}}{\rightleftharpoons}} \text{liquid crystal} \underset{(677.3\pm0.5)\ \text{K}}{\overset{T_{clr}}{\rightleftharpoons}} \text{isotropic liquid.} \quad (2)$$

This splitting, which represents another characteristic feature of potassium *n*-butanoate, was confirmed by subsequent a.c. conductance measurements by Schiraldi and Chiodelli.[9] For each bifurcated couple, however, only a cumulative enthalpy change, $(\Delta_{trs} H^\circ_m)_{cum}$, could be measured by d.s.c. because of overlapping (particularly large in the case of the couple at lower temperature) and, accordingly, only a cumulative entropy contribution $\Delta_{trs} S^\circ_{m,cum} = \Delta_{trs} H^\circ_{m,cum}/\langle T_{trs} \rangle$ {where $\langle T_{trs} \rangle = (\langle T_{trs,1} \rangle + T_{trs,2})/2$, and $T_{trs,1}$, $T_{trs,2}$ refer to component peaks 1, 2 of the couple, respectively} could be calculated. (For simplicity, only $\langle T_{trs} \rangle$ values were quoted in Paper IV[2] of this series, and phase designation was made accordingly.)

It is worth noting that for *n*-$CH_3(CH_2)_2CO_2K$, summation of d.s.c. $\Delta_{trs} S^\circ_{m,cum,III\to II+II\to I}$ (represented by a filled square in figure 1) plus $\Delta_{fus} S^\circ_m$ provides a value which lies on the extension of $\Delta_{fus} S^\circ_m$ curve for $6 \leqslant n_C \leqslant 8$ in figure 1, as does the $(\Delta_{fus} S^\circ_m + \Delta_{trs} S^\circ_m)$ value {relevant to fusion + the close-to-fusion transition mentioned above} for *n*-$CH_3(CH_2)_2CO_2K$; both values are represented by open triangles in the figure.

Finally, *n*-butanoate is the shortest member of the potassium *n*-alkanoate family which can exist as a mesomorphic liquid, and, at the same time, the homolog exhibiting the largest $\Delta_{clr} S^\circ_m$ and the smallest $\Delta_{fus} S^\circ_m$. The open squares represent in figure 1 the clearing entropies of the sequence *n*-butanoate, ···, *n*-pentadecanoate. The clearing mechanism can be reasonably assumed to be the same from n_C of 4 through 15; consequently, a single slightly curved line can be used to represent the corresponding $\Delta_{clr} S^\circ_m$ values. For the present purposes (summation; see below), separate linear interpolation for $6 \leqslant n_C \leqslant 8$, and $10 \leqslant n_C \leqslant 15$ is an alternative.

Summation of $\Delta_{fus} S^\circ_m$ and $\Delta_{clr} S^\circ_m$ values yields $\Delta_{\Sigma trf} S^\circ_m$ values. On the extension of the $\Delta_{\Sigma trf} S^\circ_m$ curve relevant to $6 \leqslant n_C \leqslant 8$ lie: (a) the values (represented by filled triangles) obtained by adding to the corresponding open triangles (lying in turn on

the extension of the $\Delta_{fus}S^{\circ}_{m}$ line) the clearing entropies pertaining to *n*-butanoate and *n*-pentanoate, respectively; and (b) the fusion entropy of the propanoate. This, on the one hand, allows one to conclude that (analogously to what we found previously[10] in the lithium family) the sequence starting with propanoate metastable for lithium and ending with the longest homolog unable to form plastic crystals (*i.e.* either *n*-hendecanoate or *n*-octanoate when the cation is either Li or K, respectively) have correlated fusion mechanisms; and—on the other hand—offers an interesting example of "stepwise fusion". Indeed, for each homolog with $3 \leqslant n_C \leqslant 8$ transformation into a clear melt of the crystalline phase stable around 500 K occurs, with an overall entropy variation $\Delta_{\Sigma trf}S^{\circ}_{m}$ almost linearly depending on n_C, in a single step (*i.e.* crystal I → isotropic liquid) when $n_C = 3$, in four steps (*i.e.* crystal III → crystal II; crystal II → crystal I; crystal I → liquid crystal; and liquid crystal → isotropic liquid) when $n_C = 4$, in three steps (*i.e.* crystal II → crystal I; crystal I → liquid crystal; and liquid crystal → isotropic liquid) when $n_C = 5$, and in two steps (*i.e.* crystal I → liquid crystal, and liquid crystal → isotropic liquid) when $n_C = 6, 7, 8$.

In the sub-ambient region (down to 110 K), the only information available prior to the present study is that partially overlapping peaks occur in d.s.c. traces at (123 ± 2) and (143 ± 2) K,[3] with a cumulative entropy variation $\Delta_{trs}S^{\circ}_{m,\,cum} \approx 0.6R$.

The present paper reports on a detailed equilibrium adiabatic-calorimetric study of n-$CH_3(CH_2)_2CO_2K$ in the temperature region below 350 K, whereas investigation at higher temperatures will be completed subsequently.

2. Experimental

The potassium *n*-butanoate used in this study was prepared by reacting (in anhyrous methanol) Fluka puriss p.a. K_2CO_3 with (5 per cent excess over stoichiometry) Fluka puriss ($\geqslant$99 per cent: tested at the source by g.c.) *n*-butanoic acid. The solid recovered after evaporation to incipient crystallization in a Rotavapor device under reduced pressure and subsequent cooling was further purified by repeated crystallization from anhydrous ethanol. After drying under vacuum at a temperature intermediate between $T_{II \rightarrow I}$ and T_{fus}, the sample was submitted to d.s.c. analysis in the superambient region: fair agreement was obtained between the traces recorded here and the values of T_{trs}, T_{fus}, and T_{clr} listed in table 1.

The salt was loaded into a gold-plated OFHC copper calorimeter, laboratory designation W–62, and the determinations were made in the Mark X cryostat described elsewhere.[11] Data logging, calorimetry, and programming were computer assisted.[12]

Two separate loadings were made of this sample because an instrumental problem resulted in the melting of a Cerroseal-soldered seam of the calorimeter. Approximately 60 d between the loadings permitted complete diagnosis and repair of the instrument. The mass of the sample used during the first loading was 24.000 g (corresponding to 0.19017 mol; molar mass: 126.201 $g \cdot mol^{-1}$, on the basis of the 1978 IUPAC relative atomic masses), that during the second loading 20.975 g ($\doteq$0.16620 mol). The buoyancy corrections were calculated using a density of

1.21 $g \cdot cm^{-3}$. The pressures of purified helium admitted into the (previously evacuated) calorimeter during the first and second loading, to promote thermal equilibrium, were 3.39 and 3.60 kPa (at room temperature), respectively.

The heat capacity of the second loaded sample was 84 per cent of the total (sample + calorimeter) heat capacity at 10 K and decreased to 55 to 60 per cent above 115 K except in the transition region.

The thermal history outlined below in linear array shows the details of the thermal cycles to which the sample was subjected: the unbroken arrows show cooling periods while dashed arrows show periods of acquisition of results. First loading:

$$297.5\ \text{K} \xrightarrow{12\ \text{h}} 161\ \text{K} \xrightarrow[\text{Series I}]{13\ \text{h}} 350\ \text{K} \xrightarrow{12\ \text{h}} 141\ \text{K} \xrightarrow[\text{no results taken}]{9\ \text{h}} 298\ \text{K}.$$

Second loading (after 64 d at 298 K):

$$298\ \text{K} \xrightarrow{16\ \text{h}} 186\ \text{K} \xrightarrow[\text{Series II}]{12.5\ \text{h}} 346\ \text{K} \xrightarrow{16\ \text{h}} 103\ \text{K} \xrightarrow[\text{Series III}]{8\ \text{h}} 212\ \text{K}$$

$$\xrightarrow{13\ \text{h}} 63\ \text{K} \xrightarrow[\text{Series IV}]{7\ \text{h}} 157\ \text{K} \xrightarrow{18\ \text{h}} 110\ \text{K}$$

$$\xrightarrow[\text{Series V}]{11\ \text{h}} 160\ \text{K} \xrightarrow{17\ \text{h}} 6\ \text{K} \xrightarrow[\text{Series VI}]{3\ \text{h}} 12\ \text{K}$$

$$\xrightarrow{0.5\ \text{h}} 6.8\ \text{K} \xrightarrow[\text{Series VII}]{14\ \text{h}} 72\ \text{K} \xrightarrow{54\ \text{h}} 63\ \text{K} \xrightarrow[\text{Series VIII}]{15.5\ \text{h}} 152\ \text{K}.$$

3. Results and discussion

The dimensionless ratios $C_{p,m}/R$ (at the mean temperature of each measurement) are listed in table 2 in chronological sequence by series. The results obtained from the first loading at $161 \leqslant T/\text{K} \leqslant 350$ are shown in this table as Series I. Repeated determinations over the same temperature interval were made for the second loading, and the relevant results were employed to obtain the thermodynamic functions in this interval since the same calorimeter was used (after repair) for the lower-temperature regions. The standard deviation of the heat capacities from the second loading was 5 per cent at 6 K, 0.3 per cent at 20 K, and less than 0.1 per cent at temperatures above 50 K.

The overall plot of $C_{p,m}/R$ against T is shown in figure 2. An expanded section which highlights the features of the curve between 100 and 160 K is depicted in figure 3.

From figure 2 it can be seen clearly that the peaks, essentially non-isothermal but predominantly first-order transformations, are followed by a diffuse anomaly (so diffused and flattened that no reliable evaluation of the entropy change involved is possible) in the heat-capacity curve. This is probably some kind of gradual (probably higher-order) transformation with maximum height at about 250 K. Such behavior is consistent with the characteristics of carboxylic-acid salts of alkali

TABLE 2. Experimental heat capacities of potassium *n*-butanoate ($R = 8.3144\ J \cdot K^{-1} \cdot mol^{-1}$)

T/K	$C_{p,m}/R$	T/K	$C_{p,m}/R$	T/K	$C_{p,m}/R$	T/K	$C_{p,m}/R$	T/K	$C_{p,m}/R$	T/K	$C_{p,m}/R$
Series I		207.62	15.853	146.79	15.419	121.48	16.721	9.73	0.220	Series VIII	
ΔH_m Detn. A		212.74	16.058	152.95	13.645	123.40	21.648	10.33	0.284	68.39	7.577
202.67	15.629	217.89	16.259	158.81	13.875	124.57	19.397	10.95	0.312	ΔH_m Detn. C	
207.72	15.822	223.03	16.496	164.44	14.091	125.93	15.678	11.59	0.364	116.5	12.230
212.87	16.030	228.18	16.703	170.08	14.341	127.27	14.493	12.21	0.417	119.93	13.308
218.02	16.254	233.33	17.027	175.71	14.596	129.08	13.760	12.85	0.476	120.64	13.694
223.17	16.477	243.87	17.324	181.35	14.814	131.41	13.305	13.49	0.536	121.08	14.464
228.32	16.668	248.98	17.518	186.99	15.028	133.70	13.389	14.27	0.610	121.50	15.382
233.47	16.891	254.13	17.766	192.63	15.306	136.43	13.508	15.17	0.713	121.90	15.941
238.63	17.088	259.29	17.929	198.28	15.530	139.54	14.919	16.07	0.805	122.29	16.574
243.78	17.321	264.45	18.154	203.93	15.749	142.30	22.151	16.98	0.908	122.66	18.403
248.94	17.499	269.63	18.279	209.59	15.991	144.27	17.444	18.11	1.044	123.00	19.416
254.10	17.714	274.80	18.430	Series IV		145.68	14.813	19.44	1.209	123.34	20.363
259.27	17.896	279.98	18.561	65.63	7.299	147.00	13.923	20.79	1.370	123.67	19.073
264.44	18.034	285.16	18.614	70.11	7.746	148.27	13.710	22.15	1.546	124.00	21.619
269.60	18.191	290.34	18.749	74.01	8.118	149.53	13.623	23.51	1.730	124.33	19.671
274.77	18.248	293.42	18.783	77.94	8.526	151.71	13.610	24.89	1.916	124.68	17.836
279.94	18.360	299.22	19.05	81.90	8.897	154.81	13.692	26.59	2.151	125.38	17.287
285.10	18.545	305.61	19.295	86.45	9.319	157.90	13.826	28.58	2.426	131.55	13.886
290.27	18.657	311.99	19.610	91.59	9.765	Series VI		30.57	2.709	138.25	13.830
295.45	18.781	318.38	19.824	96.74	10.172	8.054	0.131	32.58	3.001	139.50	13.887
300.62	18.980	324.77	20.088	101.92	10.601	8.536	0.167	34.61	3.295	139.91	14.533
305.77	19.215	331.16	20.378	107.12	11.024	9.061	0.189	37.18	3.663	140.31	15.340
310.93	19.394	337.55	20.633	112.32	11.472	9.60	0.226	40.27	4.097	140.70	15.419
316.09	19.606	343.94	20.932	$\Delta_{trs}H_m$ Detn. A		10.14	0.252	43.37	4.518	141.06	17.832
321.25	19.779	Series III		$\Delta_{trs}H_m$ Detn. B		10.68	0.297	46.51	4.950	141.41	18.630
326.41	20.008	107.83	11.026	153.80	13.645	11.22	0.337	49.69	5.366	141.74	19.783
331.56	20.287	113.85	11.643	155.92	13.721	11.77	0.385	53.35	5.833	142.05	22.016
336.71	20.468	119.17	13.516	Series V		Series VII		57.48	6.339	142.35	21.767
341.88	20.673	124.04	19.109	112.07	11.399	7.930	0.129	61.63	6.850	142.65	21.839
347.03	20.892	129.74	13.921	115.31	11.846	8.504	0.162	65.82	7.320	146.28	15.773
Series II		136.04	13.556	118.50	12.795	9.10	0.195	70.03	7.739	152.84	13.628
ΔH_m Detn. B		141.30	18.123								

metals: comparable situations, observed in lithium homologs, have already been discussed elsewhere.[10,13]

However, when *n*-$CH_3(CH_2)_2CO_2^-$ is the anion, substitution of potassium for lithium as the cation causes dramatic changes in the thermal properties of the salt (*e.g.* the presence only of gradual solid-state transitions, and direct melting of the crystal into an isotropic liquid with lithium; presence of discontinuous, in the peculiar bifurcated mode, as well as of gradual transformations, and liquid crystal formation with potassium). Indeed, for *n*-$CH_3(CH_2)_2CO_2^-$ (which is the shortest flexible carboxylate anion), paramount importance probably ought to be attached to Michels and Ubbelohde's remark:[14] "for any given carboxylate anion, ··· contact packings of oxygen atoms of the carboxy-group around an alkali cation seem to depend in a rather sensitive way not only on the cation repulsion radius, but also on the cation polarizability". We hope to be able to comment further on

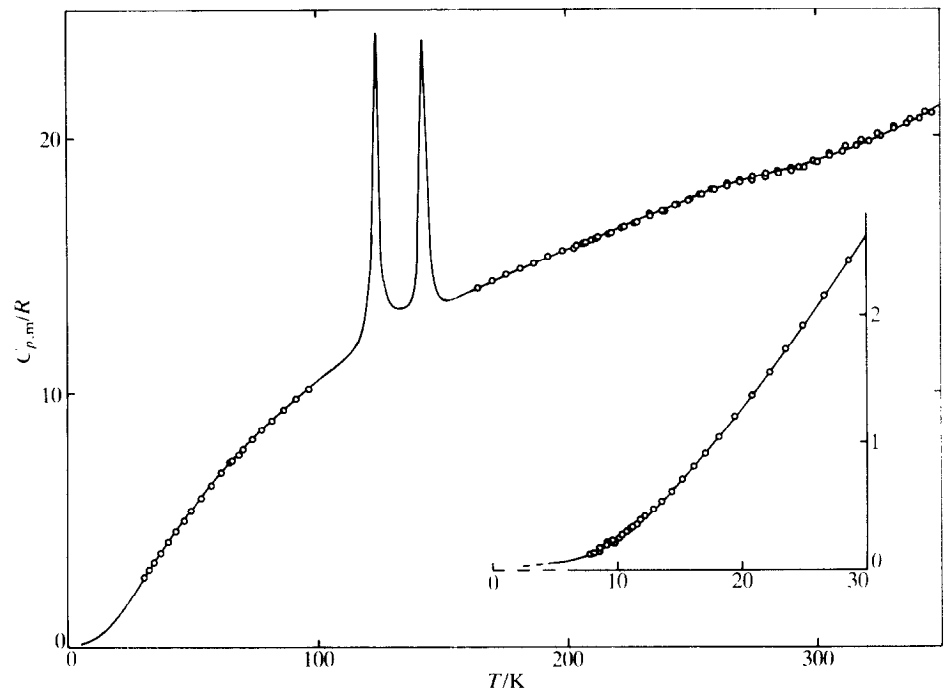

FIGURE 2. Experimental heat capacities of potassium *n*-butanoate taken in the Mark X cryostat below 350 K. The interval between 100 and 160 K (which includes the IV → III transition region) is magnified in figure 3.

TABLE 3. Enthalpy and entropy of 123.85 K transition in potassium *n*-butanoate ($R = 8.3144\ \mathrm{J \cdot K^{-1} \cdot mol^{-1}}$); N denotes the number of determintions

	N	T_1/K	T_2/K	$\Delta_{T_1}^{T_2}H_m/(R \cdot \mathrm{K})$	$\Delta_{110\,\mathrm{K}}^{135\,\mathrm{K}}H_m/(R \cdot \mathrm{K})$	$\Delta_{110\,\mathrm{K}}^{135\,\mathrm{K}}S_m/R$
			III → II Transition (123.85 K)			
Series III	4	111.13	133.19	317.51	355.8	
Series IV	2	109.71	129.69	288.29	356.2	
Series V	11	110.45	134.84	346.61	355.2	
Series VIII	16	113.60	137.22	342.76	355.3	
Graphical integration					355.5 [a]	2.901
				mean:	355.6	
Lattice contribution (estimated)					−306.3	2.501
				$\Delta_{trs}H_m/(R \cdot \mathrm{K}) =$	49.3	
				$\Delta_{trs}S_m/R$		0.400
Graphical integration				$\Delta_{trs}H_m/R$	49.24	

[a] Not included in mean value.

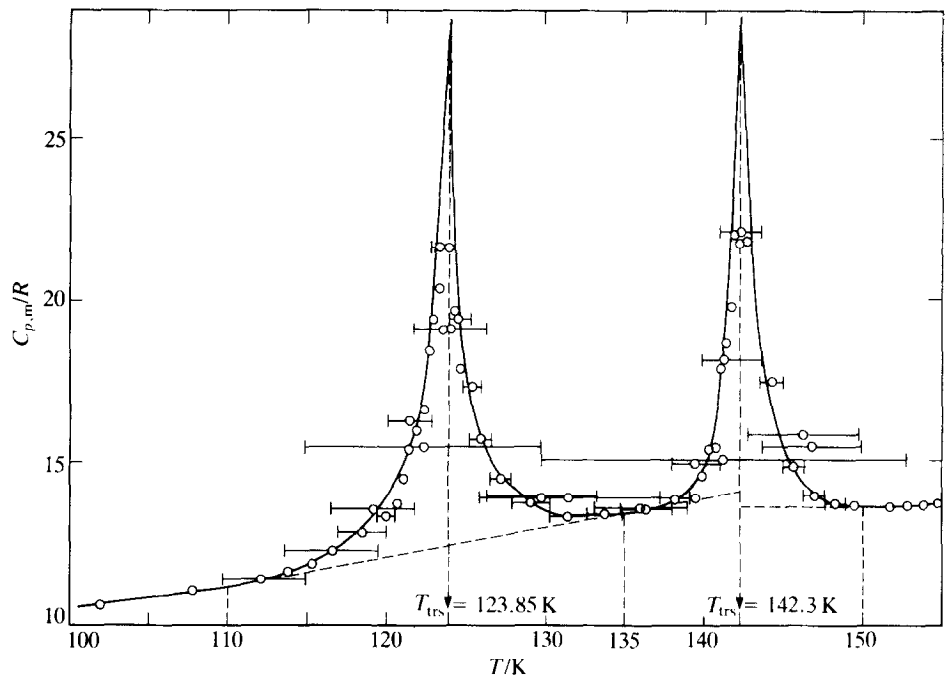

FIGURE 3. An expanded plot of experimental heat capacities of potassium *n*-butanoate through the IV → III transition region showing the temperatures of transition, the arbitrary lattice lines, and the regions over which extrapolations were made. Horizontal bars indicate the extent of enthalpy-type determinations.

TABLE 4. Enthalpy and entropy of 142.3 K transition in potassium *n*-butanoate (R = 8.3144 J · K^{-1} · mol^{-1}); N denotes the number of determinations

	N	T_1/K	T_2/K	$\Delta_{T_1}^{T_2}H_m/(R \cdot K)$	$\Delta_{135\,K}^{150\,K}H_m/(R \cdot K)$	$\Delta_{135\,K}^{150\,K}S_m/R$
			II → I Ttransition (142.3 K)			
Series III	3	133.17	149.92	261.17	238.0	
Series IV	1	129.68	152.73	346.41	238.1	
Series V	8	134.83	150.15	241.92	237.6	
Series VIII	12	137.21	149.76	203.49	236.5	
Graphical integration					237.3[a]	1.664
				mean:	237.5	
Lattice contribution (estimated)					−205.0	1.438
				$\Delta_{trs}H_m/(R \cdot K)$	32.5	
				$\Delta_{trs}S_m/R$		0.226
Graphical integration				$\Delta_{trs}H_m/(R \cdot K)$	32.3	

[a] Not included in mean value.

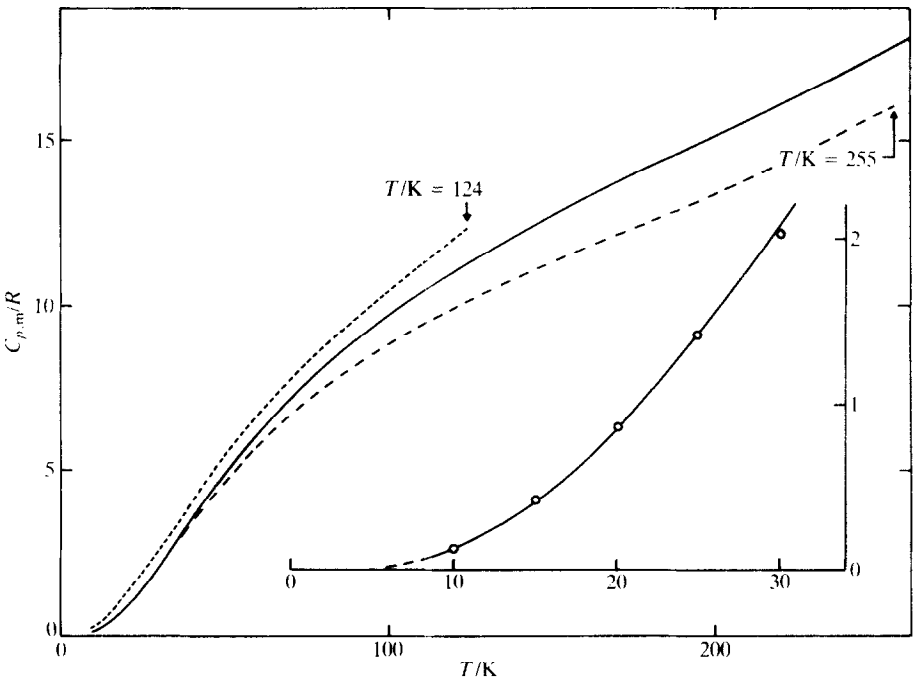

FIGURE 4. Comparison of $C_{p,m}$ taken in the low-temperature region: – – –, ○, potassium propanoate; ——, isobutanoate; – – –, *n*-butanoate.

TABLE 5. Subambient phase transitions (trs) of potassium *n*-butanoate; comparison between present and previous[3] results [a]

trs	T_{trs}/K	$\Delta_{trs}S_m/R$	$\Delta_{trs}S_{m,cum}/R$	Method
IV B → IV A	123.85	0.400	0.626	adiabatic calorimetry (this work)
IV A → III B	142.3	0.266		
III B → III A	≈250	— [b]		
IV B → IV A	123 ± 2	—	0.6	d.s.c.[3]
IV A → III B	143 ± 2	—		
III B → III A	— [c]	—		

[a] Phase designation according to scheme (2).
[b] Not evaluable (see text).
[c] Escaped d.s.c. analysis.

TABLE 6. Comparison of potassium *n*-butanoate enthalpy-type determinations with integrated smoothed heat-capacity curves (R = 8.3144 J · K^{-1} · mol^{-1})

	T_1/K	T_2/K	$\Delta H_m/(R \cdot K)$	$\int (C_{p,m}/R)dT$	$10^2\delta\Delta H_m/\Delta H_m$
A	162.09	200.21	562.09	562.4	0.06
B	186.80	205.09	281.05	281.67	0.22
C	69.34	113.62	425.79	425.33	0.11

TABLE 7. Molar thermodynamic functions of potassium *n*-butanoate:
$R = 8.3144\ \mathrm{J \cdot K^{-1} \cdot mol^{-1}}$; $\Phi_m^\circ(T, 0) \overset{\text{def}}{=} -\Delta_0^T H_m^\circ(T)/T + \Delta_0^T S_m(T)$

T/K	$C_{p,m}/R$	$\Delta_0^T S_m^\circ/R$	$\Delta_0^T H_m^\circ/(R \cdot \mathrm{K})$	$\Phi_m^\circ(T, 0)/R$	T/K	$C_{p,m}/R$	$\Delta_0^T S_m^\circ/R$	$\Delta_0^T H_m^\circ/(R \cdot \mathrm{K})$	$\Phi_m^\circ(T, 0)/R$
0	0	0	0	0		[13.40]	[12.28]	[929.50]	[5.39]
10	0.249	0.083	0.623	0.021	140	14.65	(13.18)	(1046.90)	(5.70)
15	0.690	0.260	2.885	0.068		[13.83]	[12.78]	[997.50]	[5.66]
20	1.277	0.537	7.761	0.149	142.3 [b]	(≈23.85)	(13.40)	(1078.94)	(5.82)
25	1.931	0.891	15.761	0.261		[14.03]	[13.00]	[1029.54]	[5.77]
30	2.629	1.305	27.146	0.400					
40	4.059	2.258	60.63	0.742			Phase I		
50	5.404	3.310	108.04	1.149	142.3 [b]	(≈23.85)	(13.63)	(1111.36)	(5.82)
60	6.656	4.407	168.38	1.600		[13.6]	[13.00]	[1029.54]	[5.77]
70	7.737	5.517	240.55	2.081	145	15.38	(13.89)	(1148.21)	(5.97)
80	8.716	6.614	322.80	2.579		[13.60]	[13.26]	[1066.26]	[5.91]
90	9.627	7.695	414.66	3.088	150	13.60	(14.35)	(1216.21)	(6.24)
100	10.445	8.752	515.0	3.601		[13.60]	[13.72]	[1134.26]	[6.16]
110 [a]	11.192	(9.78)	(623.25)	(4.12)	160	13.91	15.24	(1353.40)	6.78
	[11.19]	[9.78]	[623.25]	[4.12]	170	14.34	16.09	1494.7	7.299
115	11.83	(10.29)	(680.00)	(4.38)	180	14.75	16.92	1640.2	7.811
	[11.58]	[10.29]	[680.00]	[4.38]	190	15.18	17.73	1789.8	8.312
120	13.63	(10.79)	(739.00)	(4.63)	200	15.60	18.52	1943.7	8.803
	[12.03]	[10.79]	[739.00]	[4.63]	210	16.00	19.29	2101.7	9.284
123.85 [b]	(≈24.1)	(11.17)	(785.96)	(4.82)	220	16.37	20.04	2263.5	9.756
	[12.37]	[11.17]	[785.96]	[4.82]	240	17.16	21.50	2598.7	10.675
					260	17.98	22.91	2950.3	11.562
		Phase II			280	18.53	24.26	3315.8	12.421
123.85	(≈24.1)	(11.57)	(835.99)	(4.82)	298.15	19.00	25.44	3656.0	13.178
	[12.37]	[11.17]	[785.96]	[4.82]	300	19.06	25.56	3691.2	13.254
130	13.48	(12.18)	(913.15)	(5.16)	320	19.90	26.81	4080.6	14.063
	[12.93]	[11.78]	[863.75]	[5.14]	340	20.74	28.05	4486.9	14.849
135 [a]	13.40	(12.68)	(978.90)	(5.43)	350	21.21	28.65	4596.8	15.23

[a] Quantities in parentheses represent either estimated heat capacities or thermodynamic functions on the arbitrary assumption that the transitions are truly isothermal at the transition temperature indicated.

[b] Quantities in square brackets represent selected lattice heat capacities or the integrated thermodynamic functions of the selected lattice.

this point, as soon as complete thermophysical information up to the melt region is available on lithium and potassium, as well as on sodium *n*-butanoates.

Equilibrium measurements (see the expanded plot of figure 3) show that the peaks of the bifurcated transition, which appeared partially overlapping in the d.s.c. traces,[3] are satisfactorily separated. Accordingly, a separate enthalpy and entropy change can be calculated for each peak (see tables 3 and 4 for the peaks at 123.85 K and 142.3 K, respectively; calculations were performed assuming isothermal transition for each peak, as shown in figure 3).

The sub-ambient phase relations of potassium *n*-butanoate can be detailed as follows:

$$\text{Crystal VII} \underset{123.85\ \mathrm{K}}{\overset{T_{\mathrm{VII}\rightarrow\mathrm{VI}}}{\rightleftharpoons}} \text{crystal VI} \underset{142.3\ \mathrm{K}}{\overset{T_{\mathrm{VI}\rightarrow\mathrm{VB}}}{\rightleftharpoons}} \text{crystal VB} \underset{250\ \mathrm{K}}{\overset{T_{\mathrm{VB}\rightarrow\mathrm{VA}}}{\rightleftharpoons}} \text{crystal VA.} \quad (3)$$

The relevant present and previous[3] d.s.c. results are compared in table 5. When allowance is made for the combined accuracies of the techniques, the agreement can be considered to be satisfactory.

In table 6, enthalpy-type measurements are compared with the values obtained by integrating the corresponding heat capacity curves. Smoothed thermodynamic functions at selected temperatures (up to 350 K) are shown in table 7.

Finally, the heat capacities of the low-temperature phases of potassium propanoate,[1] isobutanoate,[2] and *n*-butanoate are compared in figure 4. It is interesting (see the lower right-hand corner of the figure, where the circles refer to propanoate, and the unbroken curve to isobutanoate) that at $T/\mathrm{K} < 30$ the heat capacities of the propanoate and isobutanoate are practically undistinguishable, whereas that of isobutanoate is within about 10 per cent of that of the *n*-butanoate at the upper end of the stabilization range of the latter. However, the greater molecular freedom of the latter eventually leads to large values.

REFERENCES

1. Franzosini, P.; Westrum, E. F., Jr. *J. Chem. Thermodynamics* **1984,** 16, 81.
2. Franzosini, P.; Westrum, E. F., Jr. *J. Chem. Thermodynamics* **1984,** 16, 127.
3. Ferloni, P.; Sanesi, M.; Franzosini, P. *Z. Naturforsch.* **1975,** 30a, 1447.
4. Ferloni, P.; Spinolo, G.; Zangen, M.; Franzosini, P. *Z. Naturforsch.* **199,** 32a, 329.
5. Sanesi, M.; Ferloni, P.; Franzosini, P. *Z. Naturforsch.* **1977,** 32a, 1173.
6. Cingolani, A.; Spinolo, G.; Sanesi, M.; Franzosini, P. *Z. Naturforsch.* **1980,** 35a, 757.
7. Sokolov, N. M. *Tezisy Dokl. X. Nauch. Konf. S.M.I.* **1956.**
8. Sokolov, N. M.; Pochtakova, E. I. *Zh. Obshch. Khim.* **1958,** 28, 1693.
9. Schiraldi, A.; Chiodelli, G. *J. Phys. E.: Sci. Instr.* **1977,** 10, 596.
10. Ngeyi, S. P.; Westrum, E. F., Jr.; Franzosini, P. *J. Chem. Thermodynamics* **1986,** 18, 609.
11. Westrum, E. F., Jr. *Proceedings NATO Advanced Study Institute on Thermochemistry at Viana du Castello, Portugal.* Riberio da Silva, M. A. V.: editor. Reidel. New York. **1984,** pp. 745–776.
12. Franzosini, P.; Plautz, W. A.; Westrum, E. F., Jr. *J. Chem. Thermodynamics* **1983,** 15, 445.
13. Franzosini, P.; Ngeyi, S. P.; Westrum, E. F., Jr. *J. Chem. Thermodynamics* **1986,** 18, 1169.
14. Michels, H. J.; Ubbelohde, A. R. *J. Chem. Soc. Perkin II* **1972,** 1879.